CORROSION SCIENCE AND TECHNOLOGY, Vol.31, No.6(2002), pp.454~460

Mechanism and Rates of Zinc Corrosion in Tropical Countries

I. S. Cole, W. D. Ganther, S. A. Furman, A. K. Neufeld, D. Lau, L. Chotimongkol*, C. Bhamornsut*, S. Purwardia, N. V. Hue***, and S. Bernardo******

CSIRO Building, Construction & Engineering
PO Box 56, Highett, Victoria 3190, AUSTRALIA
**TISTR, Thailand Institute of Science, Technology and Research*
196 Phahonyothin Road, Chatuchak, Bangkok 10900, THAILAND
***Corrosion Center, Mining Engineering Department, Institut Teknologi Bandung*
Jl. Ganesa 10, Bandung 40132, INDONESIA
****Institute of Materials Science, Caugiay District, Hanoi, VIETNAM*
*****ITDI DST, General Santos Avenue, Bicutan Tagig, Metro Manila, THE PHILIPPINES*

A five-nation study has investigated the rate and mechanism of atmospheric corrosion of zinc in Australia, Indonesia, Thailand, The Philippines and Indonesia. During this study, 18 sites were established in these countries including severe marine, marine, severe industrial, industrial, marine/industrial, urban and highland sites. At each location, zinc plates were exposed for three-month periods and for one year. Further, a wide range of climatic and surface response parameters was measured at each location including gaseous SOx and NOx, airborne salinity, RH and temperature, rainwater composition, surface temperature and time of wetness (TOW). Exposed plates were used to determine mass loss, the nature of corrosion products (using FTIR and SEM-EDS) and the morphology of the corrosion layers (via SEM-EDS). Laboratory experiments were also carried out to elucidate the factors controlling oxide formation and stability. Regression analysis indicated that the prime factors controlling zinc corrosion were climatic (temperature and rainfall) and surface response (TOW), and surprisingly not pollutant levels. This was despite a high levels of variation in SOx levels across the sites. The possible reasons for this observation are discussed.

Keywords : *atmospheric corrosion, zinc, TOW, marine, industrial, urban*

1. Introduction

It has long been established that industrial atmospheres can cause enhanced corrosion,[1-4] with many studies in the northern hemisphere observing a strong correlation between corrosion rate and atmospheric SO_2 level. Indeed, there is a theoretical basis for such a relation, as the absorption of sulfur dioxide should promote the acidification of moisture films. More recent work has highlighted the importance of nitric oxide and ozone in the corrosion process, and it has been postulated that these gases have a synergistic effect with sulfur dioxide.[5-7] Work by Graedel[8] and Farrow *et al.*[6] has highlighted the role of the various chemical reactions that occur in the aqueous phase between sulfur products and water. Work by Cole *et al.*[9] indicates that much of the synergy effect of other atmospheric gases may be attributed to their role in oxidising S(IV) to S(VI), and that alkali precursor gases (such as NH_3) may have a contrary effect to SO_2. Thus, the pH and aggressivity of moisture layers depends on a wider range of factors than simply SO_2, so that atmospheres with the same SO_2 may have considerable variation in their corrosivity.[9]

A recent five-nation study was undertaken by Australia, Indonesia, Thailand, the Philippines and Vietnam to gain an understanding of the relationship between pollutants and corrosion of steel and zinc in tropical countries.[10] Eighteen sites were established in industrial, marine, urban and rural locations.[10] Specimens were exposed on a three-month and yearly basis. Analysis on the basis of seasonal (three-month duration) indicated that although there was a strong correlation between steel corrosion and airborne SOx level and rainwater pH, only a weak correlation was established for zinc.[9] This low correlation was not consistent with previous work in North America and Europe.[1-5] This paper analysis data from annual exposures from

Table 1. Australian and South-East Asian sites

Location		Type	Latitude/Longitude	Salient seatures
Australia	Cowley Beach	Severe marine	17°41'S; 146°06'E	On beach facing SE
	Walkamin	Highland	17°08'S; 145°25'E	On tableland NE of Cowley Beach
Philippines	Cabuyao	Industrial	14°10'N; 121°07'E	Large industrial centre
	Bicutan	Urban	14°30'N; 121°02'E	Metro Manila
	Baguio	Highland	16°30'N; 120°33'E	1500 m above sea level
Thailand	Bangkok	Urban/industrial	13°40'N; 100°30'E	On building near major road
	Rayong	Industrial	12°41'N; 101°19'E	500 m from sea
	Phrapradaeng	Industrial	13°39'N; 100°34'E	Adjacent to river 10 km from sea
	Phuket	Marine	7°50'N; 98°20'E	On seashore
Indonesia	Lembang	Highland	6°48.6'S; 107°36.6'E	Highland central Java, 62.7 km from coast, 1100 m high
	Jebus	Marine	1°39.6'S; 105°19.8'E	Bangka Island off Sumatra, 10 m from coast
	Mentok	Industrial/marine	2°4.8'S; 105°10.8'E	Bangka Island off Sumatra, 25 m from coast
	Gresik	Coastal/industrial	7°9.6'S; 112°40.8'E	West Java, 300 m from coast
	Cikampek	Inland rural	6°24.6'S; 107°27.6'E	Java, 25 km from coast
Vietnam	Hanoi	Urban	21°01'N; 105°52'E	
	Hue	Urban	16°28'N; 107°36'E	
	Nha Trang	Marine	12°20'N; 109°00'E	
	Ho Chi Minh City	Urban/industrial	10°46'N; 106°43'E	

Table 2. Data from tropical sites

Site	Exposure date (d/m/y)	Collection date (d/m/y)	Days exposed	Season at start of exposure	Low alloy Cu steel (μm/ year)	Zinc mass loss (μm/year)	ISO TOW (% time)
Bagiou	12/7/98	16/7/99	369	End dry	13.0	2.1	80
bicatun	16/7/98	2/9/99	413	End dry	37.1	1.1	45
Cabuyao	7/7/98	8/7/99	366	End dry	41.3	1.8	52
Phrapradaeng	24/6/98	25/6/99	366	Wet	40.1	1.5	30
Rayong	30/6/98	28/6/99	363	Wet	24.9	2.6	33
Phuket	2/7/98	22/6/99	355	Wet	30.9	1.9	53
Bangkok	23/6/98	25/6/99	367	Wet	18.0	1.2	33
Cowley Beach	20/10/98	2/11/99	378	End dry	285.5	7.6	85
Walkmin	19/10/98	1/11/99	378	End dry	6.8	0.4	71
Lembang	15/3/99	4/4/00	386	End wet	6.4	0.9	62
Jebus	18/3/99	10/4/00	389	End wet	37.0	2.0	70
Mentok	17/3/99	11/4/00	391	End wet	40.1	2.7	64
Gresik	19/3/99	5/4/00	383	End wet	30.3	2.5	50
Cikampek	16/3/99	7/4/00	388	End wet	28.6	2.4	52

Site	TOW measured (% time)	SO_2 ($\mu g/m^3$)	Max. ave. daily temp. (°C)	Ave. temp. (°C)	Ave. RH (%)	Rainwater pH	Salinity ($mg/m^2.day$)	Rainfall (mm/year)
Bagiou	94	2	39.0	22	86	5.1	3	3283
Bicatun	39	21	39.7	27	78	4.2	6	2408
Cabuyao	65	14		27	75	4.6	6	2408
Phrapradaeng	61	68	38.2	30	73	6.0	6	1530
Rayong	74	15	38.1	30	70	6.0	23	1022
Phuket	67	4	38.0	30	77	5.9	87	2133
Bangkok	34	21	33.7	29	70	5.6	6	1530
Cowley Beach	94	0.8	28.7	25	80	5.4	400	3335
Walkmin	53	0.5	27.7	21	70	4.7	8	1037
Lembang	49	4	37.6	22	77	5.6	1	2062
Jebus	65	1	34.9	27	85	6.5	79	2475
Mentok	70	50	37.0	28	81	4.9	39	2475
Gresik	64	25	39.6	29	74	5.4	24	2043
Cikampek	99	19	39.6	28	73	4.8	25	2112

the same exposure program in tropical countries. Again a strong correlation between SO_2 level and corrosion rate of zinc plates is not evident. The paper reports further investigations, including simple acidified droplet experiments and oxide stability and buffering capacity experiments, aimed at elucidating more clearly the possible mechanisms controlling corrosion in tropical conditions

2. Experimental

The position and the characteristics of all sites are given in Table 1, while in Table 2 pollutant parameters, times of wetness (TOW) and mass loss data are given for one-year exposures for the majority of sites. Airborne salinity is measured using a standard wet candle technique according to ISO 9223, where NOx, SOx and HNO_3 are measured using a passive sampling technique, and TOW is measured using gold grid mounted on zinc specimen. The monsoonal periods fall between May and September/October in Thailand and Indonesia, June and August in the Philippines, and December and February in Australia. The mass loss data is determined using zinc specimens of dimensions 1 × 100 × 150 mm and with compositions as given in Table 3 exposed as per ASTM G1, or using mild steel (containing Cu) of dimensions 3 × 100 × 50 mm (density 7.764) and was exposed vertically. The composition of the steel is given in Table 4. For selected rainwater samples, anion and cation concentrations were obtained (using ion chromatography) and are given in Table 5.

Table 3. Composition (%) of zinc

Cu	Ti	Fe	Cd	Pb	Sn	Al	Zn
0.064	0.006	0.003	0.002	0.001	0.001	<0.001	Remainder

Table 4. Composition (%) of low alloy Cu steel

C	P	Mn	Si	S	Ni	Cr	Mo	Cu	Fe
0.166	0.004	0.602	0.057	0.002	0.285	0.13	0.01	0.235	Remainder

Table 5. Rainwater - average composition over one year

Site	Na	K	NH_4	Ca	Mg	Cl	NO_2	NO_3	PO_4	SO_4
Bagiou	0,51	2,09	1,14	0,90	0,00	1,88	0,00	0,00	0,28	1,94
Bicutan	0,47	0,85	0,66	1,40	0,12	1,33	0,01	1,53	0,84	3,02
Cabuyao	0,30	1,06	1,26	0,79	0,11	1,27	0,01	0,55	0,05	3,20
Cowley Beach	25,81	1,45	0,57	1,81	2,70	49,99	0,00	3,40	0,51	6,37
Walkamin	1,63	1,40	1,02	0,38	0,14	2,56	0,00	2,20	0,58	0,94

2.1 Surface analysis

All plates (both seasonal and yearly exposures) were examined by Fourier transform infra-red spectroscopy (FTIR).[11] Species identified were always zinc hydroxy carbonate, chloride or sulfate, with results being given in Table 6. Scanning electron microscopy (SEM) was also used to examine specimens. Examination was carried out on both the surfaces on the specimen and on cross sections through the sample.

A number of characteristic patterns were observed during examination of the corroded surfaces. On speci-

Table 6. FTIR of annual and seasonal exposures

Location	Summer	Autumn	Winter	Spring	Annual
Cowley Beach	CO_3/Cl	CO_3/Cl	CO_3/Cl	CO_3/Cl	CO_3/Cl
Walkamin	CO_3	CO_3	CO_3	CO_3	CO_3
Cabuyao	CO_3/SO_4	CO_3/SO_4	CO_3/SO_4	CO_3/SO_4	CO_3/SO_4
Bicutan	SO_4	CO_3/SO_4	CO_3	CO_3/SO_4	CO_3/SO_4
Baguio	CO_3	CO_3	CO_3	CO_3	CO_3
Bangkok	SO_4/CO_3	CO_3/SO_4	CO_3/SO_4	SO_4/CO_3	CO_3/SO_4
Rayong	CO_3/Cl	CO_3/SO_4	SO_4/Cl	CO_3/SO_4/Cl	CO_3
Phrapradaeng	SO_4	CO_3/SO_4	CO_3	SO_4/CO_3	CO_3/SO_4
Phuket	CO_3/SO_4/Cl	CO_3/SO_4	CO_3	CO_3/SO_4/Cl	CO_3/Cl
Lembang		-	CO_3	CO_3	-
Jebus	CO_3	CO_3	CO_3	CO_3	CO_3
Mentok	CO_3/SO_4	CO_3/SO_4	CO_3/SO_4	CO_3/SO_4	CO_3/SO_4
Gresik	SO_4/CO_3	SO_4	SO_4	SO_4	SO_4/CO_3
Cikampek	CO_3		CO_3	SO_4	-
Hanoi	CO_3	CO_3	CO_3	SO_4	CO_3
Hue	-	CO_3	-	CO_3	CO_3
Nha Trang	-	Cl/CO_3	CO_3/Cl	CO_3/Cl	CO_3
Ho Chi Minh City	CO_3/SO_4	SO_4/CO_3	SO_4/CO_3	CO_3/SO_4	CO_3/SO_4

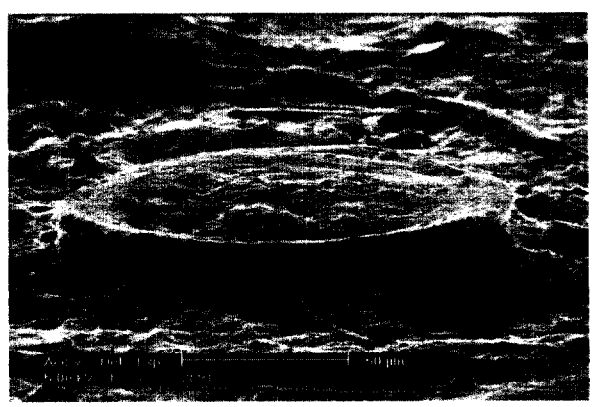

Fig. 1. Pedestal formation observed at Phuket

Fig. 2. Dissolution pits observed at Nha Trang

Fig. 3. S-containing formations at Bangkok

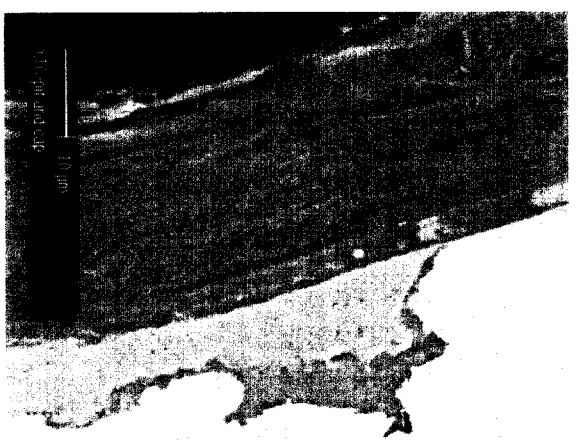

Fig. 4. Pit below pedestal at Cowley Beach

mens exposed to marine environment a typical formation was the pedestal, previously reported by Neufeld and Cole[12] and presented in Fig. 1. The distribution of these morphologies on the surface of the specimens is very regular, and in some cases there may be as many as 2 or 3 in an area of 500 × 500 microns. Typically the diameter of the morphology is about 100 microns, however sizes range from 50 to 250 microns in diameter. EDS analysis indicated that the surface of the pedestal is composed of zinc hydroxy carbonate. In other regions dissolution of the zinc hydroxy carbonate oxide is clearly evident, as in Fig. 2. Such dissolution pits with diameters of 25-100 μm are frequent on all tropical marine exposures.

At industrial sites such pedestal formation is not evident and the surfaces appear more regular. However, a number of features are apparent, including islands of sulfate-rich crystalline lattice structures, and other formations of dimensions 50-200 μm, as shown in Fig. 3 The oxide at the centre of this formation is likely to be a mixed zinc-hydroxy carbonate and sulfate. Finer craters with dimensions from 1 to 5 μm are also apparent.

2.2 Cross-sections

Examination of the cross-sections reinforced and refined the information obtained from the surface examinations. The specimens exposed to marine conditions showed very irregular oxide layers, containing both pedestal and dissolution areas. Further, the oxide was frequently cracked and contained numerous pores. An interesting observation is that below or adjacent to the pedestal formation, large pits (often nearly occluded) were frequently found. Fig. 4 shows such a pit from a specimen exposed at Cowley Beach

For the non-marine sites, the oxide surface was much smoother, without any indication of significant pores or cracking. A number of features reflecting observations of the surface specimens were apparent. Small dissolution zones in the oxide of around 1-5 μm were frequently observed, whilst areas of oxide build up and metal attack frequently had dimensions of the order of 50 μm or more. Observations from the cross-sections of the one-year exposed specimens are summarised in Table 7 using the key in Table 8 to define the significance of the ratings. The aspect ratio of the pit is defined as pit width:depth.

2.3 Regression analysis

On the basis of data in Table 2, regression analysis was used to derive the best parametric models to describe the variation in zinc and steel corrosion rates. In addition to the variables in this table, the average hydrogen ion concentration in μm in rainwater ($[H+]_{conc}$) and average total hydrogen ions in rainwater per day were derived and used in the regression analysis. The most appropriate models were:

Table 7. Observations from SEM cross-sections

Site	SO_2 ($\mu g/m^3$)	Zinc mass loss (μm/year)	Type of S,Cl distribution	Range of oxide thickness	Form of pit	Pit depth range
Phrapradaeng	68	1.5	1	1	1	1
Mentok	40	2.7	2	1	1	2
Gresik	30	2.7	3	2	1	1
Bangkok	21	1.2	1	1	2	2
Bicutan	21	2	2	1	2	4
Ho Chi Minh	20		1	2	1	1
Rayong*	15	2.6	1	2	1	1
Cabuyou	14	1.8	2	1	2	3
Hanoi	5	1.3	3	1	3	4
Lembang	4	0.9	2	2	2	3
Bagiou	2	2.1	4	1	2	4
Walkamin	0.5	0.8	4	1	2	3
	Salinity (mg/m^2.day)					
Nha Trang			1	4	3	3
Jebus	47	2.0	4	4	3	3
Rayong	23	2.6	4	3	2	3
Phuket	87	1.9	4	3	2	3
Cawley	400	7.6	3	5	3	4

Table 8. Key to ratings used in Table 7

Class	Pit form (aspect ratio)	S,Cl distribution in oxide	Pit depth (μm)	Oxide thickness (μm)
1	Very Shallow pit(>1.5:1)	Even Distribution	(P)<5	(T)<5
2	Sharper pits (1.5:1 to 1:2)	Throughout but concentrated at the bottom of pits	2<P<5	5<T<10
3	Nearly Occluded Pit	Only at the bottom of pits	5<P<10	10<T<20
4		Not found	10<P<20	20<T<80

For zinc: Mass loss = δ T^{α} R^{β} TOW^{χ}

where T is average temperature, R is average rainfall, TOW is time of wetness, and α, β, χ and δ are the regression constants having values of 2.8, 0.57, 0.88 and 0.15 respectively.

For steel: Mass loss = η (salinity + 1.5 × $[H+]_{conc})^{\varepsilon}$ T^{ϕ} RH^{γ}

where ε, ϕ, γ and η are constants having the values 0.2, 4.8, 2.6 and 0.041 respectively.

The R-sq. (adjusted for d.f) for the zinc and steel models are 0.82 and 0.85 respectively.

When the formulae in Haagenrud and Henriksen[7] or Tidblad *et al.*[4] are applied to the data from non-marine sites in Table 2 to derive zinc mass loss, both data formulae give average corrosion rates of between 1 and 2 μm/year which is within the observed range. However, both these formulae have a strong dependence on SO_2 and so, not surprisingly, the fit to these formulae is very poor.

3. Subsidiary experiments

3.1 Droplet experiments

In these experiments, a 0.5 ml droplet of electrolyte was placed on a zinc plate within a constant humidity chamber where the RH was 95% and temperature was 23 ℃. The pH at the centre of the droplet was monitored using a micro-pH meter. Prior to testing the zinc plate was cleaned with distilled water and alcohol. The droplet had variable pH, controlled by the addition of sulfuric acid, and varying base composition from deionised water, 5% NH_4SO_4 and 0.1 and 1 M NaCl solution. In Table 9 the major details of each experiment are listed, including the initial solution pH, the lowest pH reached on the plate (this generally happened almost immediately after contact between droplet and plate), the highest pH (generally occurred towards the end of the time) and the time taken to reach pH of 3, 4, 5 and 6.

The solubility and stability of the various zinc hydroxy anions have been determined. The results in Fig. 5 show that the pH range over which the zinc hydroxy anions become soluble, measured by two techniques, is between

Table 9. Key features of droplet experiments

Solution	Solution pH	Lowest pH	Time(min) that pH is less than				Highest pH
			3	4	5	6	
Deionised water	3.0	0.4	20	30	40	50	7.4
5% NH_4SO_4	2.9	2.6	50	95	105	115	6.7
0.1 NaCl	3.1	2.9	4	30	60	90	7.4
1 M NaCl	3.0	0.8	14	20	26	35	6.6
Deionised water	3.9	3.2	-	12	22	35	8.4
0.1 NaCl	4.1	0	8	12	18	28	7.6
Deionised water	5.0	5.0	-	-	-	12	7.3
0.1 NaCl	5.0	0.8	14	20	26	35	6.6

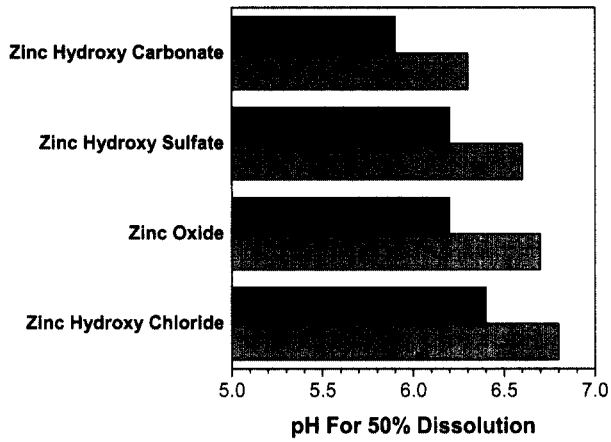

Fig. 5. pH stability of zinc hydroxy anions using two techniques

5.8 and 6.8. Zinc hydroxy chloride is the least stable and zinc hydroxy carbonate is the most stable. In addition, all of these solid compounds exhibit a strong buffering capability when exposed to acidic conditions. This makes it very difficult to change the pH of suspensions of these solids and a large excess of acid is required before the solids begin to dissolve.

4. Discussion

It is useful to define a sequence of events from pollutant deposition to surface degradation based on the presented data. Plates are likely to be wet around 50% of the time for non-marine sites and considerably in excess of this for marine sites. For non-marine sites, periods of wetness are during the night and during rain spells. During the day, surface temperature of the plates is quite high, so that moisture films or droplets quickly evaporate. In marine locations, due to the high levels of hygroscopic salts, moisture layers persists for longer periods despite high surface temperatures.

Deposition onto surfaces may be either by aerosol deposition, gaseous deposition onto a moisture film, gaseous deposition onto a dry surface, or deposition by fog or rain droplets. In all cases except gaseous deposition onto a dry surface, the nature of the chemistry of the aerosol or the moisture film or droplet depends on the nature of the gaseous species present in the atmosphere and their gaseous/aqueous phase interactions. Cole *et al.* [9] modelled this. Although gaseous SO_2 levels control the chemistry of moisture films or droplets, it is also heavily influenced by oxidisers of SO_2 in solution and by alkali precursors (e.g. NH_3). For the limited data rainwater analysis does indicate significant ammonia ions, with the non-marine sites having ammonia to sulfate ratios from 1:1 to 1:4. These levels could certainly effect the pH of rainwater and not surprisingly the rainwater pH details in Table 2 were quite benign.

It is observed that all plates form continuous oxide layers before the end of the seasonal exposures, and that these oxides are predominately zinc hydroxy carbonate with some zinc hydroxy sulfate and zinc hydroxy chloride in industrial and marine locations respectively (see Table 5). As indicated by stability data, zinc hydroxy carbonates, and to a lesser extent, zinc hydroxy sulfates, will be reasonably insoluble in most of the rainwaters sampled in this survey. However, some dissolution of the zinc hydroxy chloride is expected, as evidenced in SEM observations and by the rarity of compounds identified in FTIR spectra from plates exposed at marine sites. In addition, data indicates that the zinc hydroxy compounds have a strong ability to buffer solutions, so acidified droplets have only a limited effect on promoting dissolution of the oxide film.

The acidified droplet experiments are extremely interesting but difficult to interpret. One conclusion is clear - the electrochemical process may significantly affect the pH of droplets and this effect is most rapid for droplets of higher pH. Thus, even on 'fresh' zinc, droplets will only remain aggressive for limited periods. The initial acidity of the droplet may degrade the plate either by promoting electrochemical activity or by degrading the oxide film. In this regard, the very low pH values obtained on plate surfaces with droplets of initial pH of around 3 may be quite significant.

SEM analysis of cross-sections reveal that three forms of corrosion are detected: shallow pits, sharp pits and 'necked' pits. Interestingly, the shallow pits occur at high SO_2 levels and the sharp or necked pits occur at moderate or low SO_2 levels or marine locations. In industrial environments where shallow pits occur, SO_4 is found throughout the oxide, but where sharp pits occur it is found mainly or only at the bottom of such pits. This somewhat surprising trend is consistent with the model of Sato.[13] In discussing iron-group metals, Sato indicated that there are two modes of pitting corrosion. One is pitting dissolution 'in the polishing state' which proceeds at more noble potentials, and the other is in the active state which proceeds at less noble potentials. Increasing ion concentrations and reduced cathodic areas stabilise the region of polishing state stability, whilst larger cathodic regions and lower pH promote the active state. If an acidic droplet rich in sulfate lands on a zinc plate that is already covered with an oxide film, then following Sato's model it may be that a high sulfate level and reduced cathodic area (due to diffusion limits by the oxide) promote the 'polishing

state' and shallow pits result. In contrast, when the sulfate concentration is lower, the general corrosion zone passivates as sulfate precipitates out of solution. Corrosion will only recommenced if a localised area of higher susceptibility (ground boundary etc) is attacked, in which case the microstructure feature promotes a sharp pit which will lead to a lowering of the local pH and a prolonged active corrosion period. However, at some stage the pit will cease either because of depletion of the active species or due to diffusion limits.

In the case of specimens at marine sites, the drops may be separated into two zones, with anodic activity occurring at the centre and cathodic activity in the 'secondary spreading'[14] area at the drop edge. Because of this large cathodic area, the active corrosion mode of Sato is promoted and very substantial corrosion products build up outside necked pits. Eventually, however, pitting stops, probably due to either diffusion limits or the reduction of the cathodic activity by these corrosion products.

The lack of a strong dependence on SO_2 levels in the zinc mass loss may be associated with a number of factors, including:

- the nature of other gaseous species;
- the effect of the nature of moisture films and rain events;
- the nature of oxides developed; and
- the effect of temperature.

These factors are connected. The acidity of aerosol and rain may be limited due to the effect of other atmospheric gases. Drops or aerosols of limited pH will have a restricted ability to dissolve the existing oxide. This limited ability will be further restrained by the stability and buffering capacity of zinc hydroxy carbonates in particular. The electrochemical process itself will lead to changes in droplet pH, so the period of attack will not be the TOW of the plate but a much smaller initial interval.

An additional contribution is highlighted by Svensson and Johansson[15] who provide an interesting perspective on the possible effect of temperature on SO_2-induced corrosion. They demonstrated that the deposition rate of SO_2 onto zinc in humid air is highly dependent on temperature, with the rate at 30 ℃ being less than one-third of that at 4 ℃.

5. Conclusions

A study across five nations in tropical regions measured zinc and steel mass loss as well as a range of climatic and pollutant factors. The study found that:

- Regression models derived to explain the variation in zinc corrosion rate did not show a dependence on atmospheric SO_2 level. In contrast, models derived for steel did show a dependence.
- Although a definitive conclusion could not be reached, possible reasons for this lack of dependence include:
  - the relatively high pH of rainwater (and probably aerosols) due to the effect of other gases species; and
  - the stability and buffering capacity of oxides formed in service.

Acknowledgments

This work is being supported by GOGAS's interim project of Managing Strategy for Pipelines Having Coating Defects and the support by National Research Laboratory Program of The Ministry of Science and Technology is acknowledged.

References

1. L. Atteraas and S. Haagenrud, in *Atmospheric Corrosion* (W.H. Ailor, ed.), John Wiley & Sons, New York, 873-891 (1982).
2. M. Benarie and F. L. Lipfert, *Atmospheric Environment*, **20**(10), 1947-1958 (1986).
3. J. W. Spence and F. H. Haynie, in *Corrosion Testing and Evaluation: Silver Anniversary Volume*, ASTM STP 1000, ASTM, Philadelphia, 208-224 (1990).
4. J. Tidblad, A. A. Mikaliov and V. Kucera, in *Proceedings of the UN/ECE Workshop on Quantification of Effects of Air Pollutants on Materials, Berlin*, p.77 (1998).
5. J. E. Svensson and L. G. Johansson, *J. Electrochem. Soc.*, **140**, 2210 (1993).
6. L. A. Farrow, T. E. Graedel, and C. Leygraf, *Corr. Sci.*, **38**(12), 2181 (1998).
7. S. E. Haagenrud and J. F. Henriksen, in *Durability of Building Materials and Components 7 (Volume One)* (C.Sostrom, ed.), E & F Spon, London, 210-218 (1996).
8. T. E. Graedel, *Corr. Sci.*, **38**(12), 2153 (1998).
9. I. S. Cole, *in Marine Corrosion in Tropical Environments*, ASTM STP 1399, S.W. Dean, G. Hernandez-Duque Delgadillo and J.B. Bushman (Eds.), ASTM, Philadelphia (2000).
10. I. S. Cole, A. K. Neufeld, P. Kao, W.D. Ganther, L. Chotimongkol, C. Bharmornsut, N.V. Hue, and S. Bernardo, *Proceedings of the 14th International Corrosion Congress, Cape Town, South Africa, 27 September to 1 October 1999*, Paper 265.2 (CD-ROM).
11. A. K. Neufeld and I. S. Cole, *Corrosion*, **53**(10), 788 (1997).
12. A. K. Neufeld and I. S. Cole, The 198th Meeting of The Electrochemical Society, Phoenix, Arizona, 22-27 October 2000, Paper F1-0449.
13. N. Sato, *Corr. Sci.*, **37**(12), 1947 (1995).
14. A. K. Neufeld, I. S. Cole, A. Bond, and S.A. Furman, *Corr. Sci.* (in press).
15. J. E. Svensson and L. G. Johansson, *Corr. Sci.*, **38**(12), 2225 (1996).